

Observation of multiphoton detachment of the H^- ion

C. Y. Tang, P. G. Harris, A. H. Mohagheghi, and H. C. Bryant
The University of New Mexico, Albuquerque, New Mexico 87131

C. R. Quick, J. B. Donahue, and R. A. Reeder
Los Alamos National Laboratory, Los Alamos, New Mexico 87545

Stanley Cohen
Cohen Mechanical Design, Broomall, Pennsylvania 19008

W. W. Smith
The University of Connecticut, Storrs, Connecticut 06268

J. E. Stewart
Western Washington University, Bellingham, Washington 98225
 (Received 21 February 1989)

We have observed nonresonant multiphoton electron detachment of H^- ions in moderately intense (a few tens of GW/cm^2) laser fields. A well-collimated beam of H^- ions with an energy of 581 MeV was intersected by focused 10.6- μm radiation from a pulsed CO_2 laser. The center-of-mass photon energy was tuned using the relativistic Doppler shift so that the minimum number of simultaneous photons required for electron detachment ranged from three to sixteen. Definite signals were observed for the minimum photon number ranging from three to eight. Our preliminary results show evidence for structure in the relative total cross section.

Multiphoton ionization (MPI) of the negative hydrogen ion has recently attracted much attention.¹⁻⁵ H^- has several characteristics that make it an especially interesting system with which to investigate multiphoton-absorption physics. A low electron affinity (0.754 eV) means that MPI can take place with photons of much lower frequency than typical MPI experiments with neutral atoms; thus ponderomotive forces (which are proportional to the intensity divided by the squared frequency) can lead to potential energies larger than not only the photon energy being used but also the electron affinity. The absence of intermediate states has the effect of simplifying the absorption process in one-electron MPI, as there are no resonance-induced effects. Furthermore, because the departing electron is subject to a short-range potential rather than a long Coulombic tail, the above-threshold ionization (ATI) process⁶ will probably be significantly altered. Finally, electron correlation is important in the description of H^- electronic states,⁷ thus allowing the possibility of examining electron correlation effects in the MPI process.

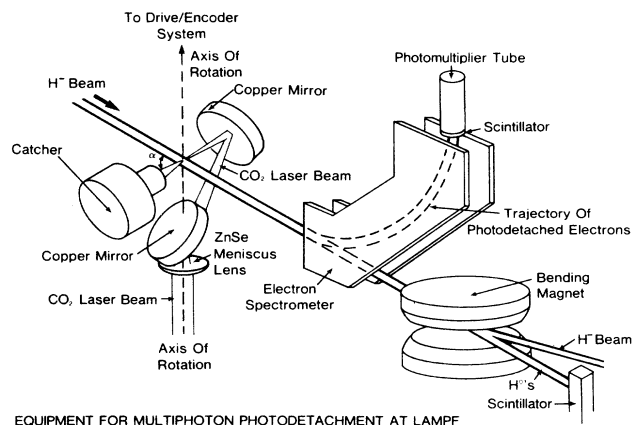
We have observed multiphoton photodetachment of the H^- ion. Using the relativistic ($\beta=0.786$) kinematics of a high-quality H^- beam at the Los Alamos Clinton P. Anderson Meson Physics Facility (LAMPF), the barycentric photon energy of a CO_2 transversely excited atmospheric (TEA) laser (Tachisto M215 oscillator, Lumonics K-103 amplifier) was Doppler tuned between 0.05 and 0.32 eV, according to the formula

$$E = \gamma(1 + \beta \cos \alpha) E_0,$$

where E_0 (0.117 eV) is the lab photon energy, γ and β are

the usual relativistic parameters, and α is the angle of intersection of the two beams such that $\alpha=0$ is head on. Thus, the minimum number of photons required to remove the outer electron from H^- can be varied from three to sixteen. This ability to tune a fixed-frequency laser over a wide range of photon energies in a simple, well-defined manner, which we believe to be unique to this experiment, allows us to examine MPI processes of many different orders.

A schematic diagram of the experimental apparatus is shown in Fig. 1. The pulsed laser beam [1.0 J/pulse, 50 ns full width at half maximum (FWHM), 0.5 pulses/s] enters the scattering chamber along the axis of rotation of the mirror system. After passing through a ZnSe men-



EQUIPMENT FOR MULTIPHOTON PHOTODETACHMENT AT LAMPF

FIG. 1. Schematic of experimental apparatus.

iscus lens ($f = 25.4$ cm), it is reflected off axis by the first of two copper mirrors; the second mirror brings it back to the rotation axis so as to intersect the H^- beam at any angle from 21° to 159° . The polarization of the light is linear, and its direction rotates with the mirror system; reflection from the copper mirrors introduces a slight ellipticity, but the relative phase change of the two orthogonal field components does not exceed 4° . The diameter of the focal region ($\approx 300 \mu\text{m}$) is much smaller than that of the H^- beam (≈ 3 mm). The waist of the focused laser beam, of area approximately 10^{-3} cm^2 , passes through the interaction point, with an intensity there of $2 \times 10^{10} \text{ W/cm}^2$ in the lab frame. A stray magnetic field of approximately 3 G in the interaction region, yielding a motional field of 1 kV/cm, was present; its effect is expected to be immeasurable, since it is much smaller than the amplitude (a few MV/cm) of the laser field.

The photodetached electrons continue to travel along with the neutral hydrogen atoms and H^- ions, until they reach the electron spectrometer; the magnetic field then sweeps them out of the main beam and into a scintillator, where they are detected in coincidence with the laser pulse.

A horizontal bending magnet farther downstream steers the primary H^- beam into a Faraday cup. The H^0 atoms continue undeflected into another scintillator, where they are detected in a time interval, the data gate, that requires them to have been produced in coincidence with the laser pulse.

Background count rates, mainly due to stripping of H^- ions by the residual gas, are measured for the H^0 signals by opening a background gate, of equal duration (500 ns) to the data gate, but delayed by $1.2 \mu\text{s}$ to ensure that no laser produced particles are present.

Starting at a center-of-mass photon energy of 0.32 eV and tuning downwards in energy, we saw photodetachment with, successively, a minimum of three to five photons before the signal was lost in the noise; by then increasing the gain on the photomultiplier tube, we were able to see photodetachment with up to a minimum of eight photons by tuning downwards in energy from 0.18 eV eV. Both of these sets of data are displayed in Fig. 2; the relative scaling between them is arbitrary.

To examine the effect of intensity on the yield, we reduced the laser-pulse energy by a factor of 2. The results shown in Fig. 3 are significantly different from those of Fig. 2; in particular, a second "dip," in addition to that already seen at 0.32 eV, appears around the nominal three-photon threshold (0.251 eV), which is in qualitative agreement with a recent theoretical prediction⁸ except that the ponderomotive potential ($E_p = e^2 E^2 / 4m\omega^2$, where e and m are the electron charge and mass, E is the electric field amplitude, and ω is the angular frequency of light) may have added to the ionization threshold, shifting the expected threshold position.^{4,9} For an intensity of 20 GW/cm^2 the ponderomotive energy is 0.21 eV; it is then possible that the dip around 0.32 eV may reflect the transition from a four-photon to a three-photon process. However, the peak intensity of the laser pulse may be considerably higher than this; the temporal variation in intensity, as measured with a fast pyroelectric detector, is

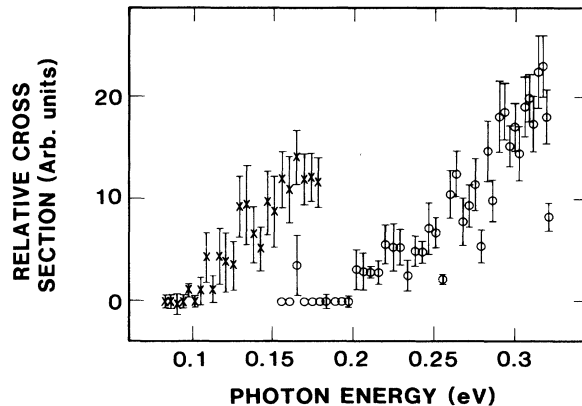


FIG. 2. Relative total cross section for multiphoton detachment of H^- as a function of photon energy, from 0.15 to 0.32 eV, and from 0.08 to 0.18 eV (obtained with a higher photomultiplier gain), using a laser pulse energy of 1.0 J. Y-axis scaling in the two sets of data is different. The error bars are statistical only; they represent the standard deviation of the mean number of signal counts per laser shot, measured over the fifty or so laser shots.

shown in Fig. 4. We may therefore expect to see large ponderomotive shifts, of the order of the ionization potential itself. If the ponderomotive energy is as high as 0.84 eV, the thresholds for six-, seven-, eight-, and nine-photon detachment fall, respectively, at 0.318, 0.265, 0.227, and 0.199 eV, which are positions of approximate minima in Fig. 3. Both of the peaks shown in Fig. 3 are strongly suppressed due to saturation of an analog-to-digital converter (Lecroy ADC-M2249A).

Since we do not know the geometry of the beam overlap—either temporal or spatial—very well, we are able to calculate cross sections only roughly. We present here our preliminary data; these have been normalized by the inclusion of a factor $\sin\alpha/(1 + \beta\cos\alpha)$, which accounts for the changing overlap of two cylinders as the angle of intersection changes, as well as for the relativistic variation

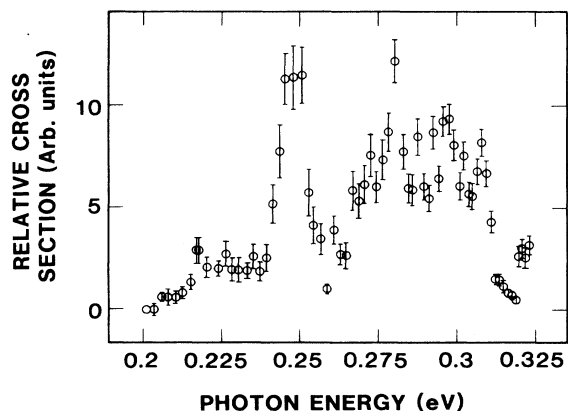
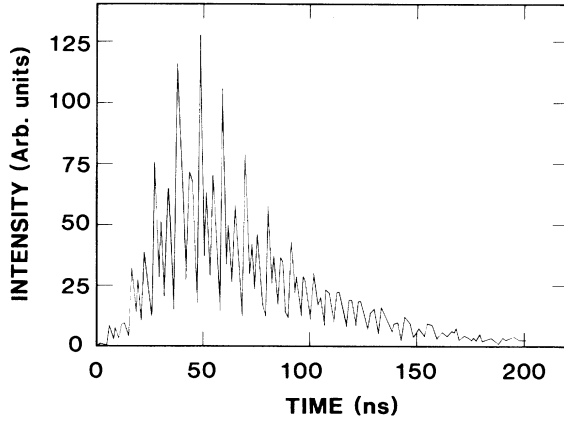


FIG. 3. Relative total cross section for multiphoton detachment of H^- as a function of photon energy, using a laser pulse energy of 0.5 J.


 FIG. 4. Temporal profile of CO₂ laser pulse intensity.

of intensity with angle. A simple derivation of this factor follows.

For an n th-order multiphoton process well below saturation, the transition rate per atom is given by¹⁰

$$W'_n = \sigma_n (F')^n,$$

where F is the photon flux, σ_n is the generalized cross section, and the prime indicates the rest frame of the ion. If higher-order processes also contribute, we may write the transition rate as

$$W' = \sum_{m \geq n} \sigma_m (F')^m = \sigma F',$$

where σ is the total cross section:

$$\sigma = \sum_{m \geq n} \sigma_m (F')^{m-1}.$$

The total number of counts per micropulse is therefore given by

$$N' = \int \int dV' dt' \rho' \sigma F',$$

where the integrals cover the interaction volume and time (one micropulse of the H⁻ beam) of the photon and atomic beams, and ρ is the density of H⁻ ions. Since the total number of counts is invariant, density ρ transforms as $\rho' = \rho/\gamma$, $dV' dt' = dV dt$, and photon flux $F = I/E$ transforms as photon energy to the first power,¹¹ i.e., $F' = F\gamma(1 + \beta \cos \alpha)$, we have

$$N = \int \int dV dt (1 + \beta \cos \alpha) \sigma \rho F.$$

In a real situation, H⁻ ions traversing the interaction region at different positions and times may see varying fields, as a result of the spatial and temporal distribution of the laser intensity. Let us, however, assume that the interaction volume is a cylinder, corresponding to that part of the focus of the laser beam which lies within the H⁻ beam; assume also that the laser beam is uniform in intensity and in time within this cylinder. Then, the last equation simplifies to

$$N = V_0 T_0 \rho \sigma F \frac{1 + \beta \cos \alpha}{\sin \alpha},$$

where T_0 is the time of interaction of the beams, and V_0 is the interaction volume at $\alpha = 90^\circ$. We may then obtain the relative cross section:

$$\sigma \propto \frac{N \sin \alpha}{F(1 + \beta \cos \alpha)}.$$

The lowest possible order of the multiphoton process is determined in part by the ponderomotive potential. Rather conveniently, as this is proportional to the intensity divided by the square of the frequency, it is independent of angle, and therefore of photon energy, in our experiment. Unfortunately, we have as yet no means of determining the energies of the photodetached electrons, and so we are unable to calculate the order of the process; but if, in fact, the lowest-order process is dominant, we have, in terms of the generalized cross section,

$$\sigma = \sigma_n (F')^{n-1} = \sigma_n F^{n-1} \gamma^{n-1} (1 + \beta \cos \alpha)^{n-1},$$

and so

$$\sigma_n \propto \frac{N \sin \alpha}{[F\gamma(1 + \beta \cos \alpha)]^n},$$

where the photon flux F is approximately 1.1×10^{30} photons/cm²s. Using our estimates of $V_0 = 3 \times 10^{-4}$ cm³, $T_0 = 1$ ns, and $\rho = 1200$ H⁻/cm³, a typical 40 counts per micropulse for a four-photon process yields a total cross section $\approx 10^{-19}$ cm² and a count rate per atom (barycentric frame) of order 10^{11} /s, in good agreement with the theoretical predictions in Ref. 4.

The curves presented here cannot claim to be a truly accurate representation of the relative cross section. The primary aim of this experiment was to find a signal for multiphoton photodetachment, to justify a large-scale, thorough investigation; however, inherent weaknesses in the design of the equipment meant that certain systematic errors were impossible to overcome. These include the following.

(1) Precision optical alignment was impossible, and the focal spot "wandered" by about 1 mm vertically as the mirror system rotated through 180°. This changed the effective overlap, which was optimized at a particular angle by vertical steering of the (3-mm-wide) H⁻ beam.

(2) The incident laser beam was convergent, forcing the waist of the focused beam to fall slightly short of the axis of rotation. Although compensated for to some degree by steering the H⁻ beam, this may have caused angular variations of laser-beam intensity that have not been allowed for in the yield curves.

(3) The time structure of the laser beam was not smooth. The H⁻ beam came in 1-ns-wide pulses, spaced 100 ns apart; these "micropulses" could encounter either dips or peaks in laser intensity, although these would tend to average out over the sixty or so laser pulses used for each angle in the longer scans.

(4) At small angles, and therefore high photon energy, the higher cross section, larger volume of overlap, and higher effective intensity combined to produce a count rate sufficient to approach saturation in our detectors. The cross sections shown may therefore be slightly suppressed towards the high-photon-energy end of the scale.

(5) A small divergence introduced to the laser beam by

the focusing element limits the angular resolution of the system to 2.5° ; this gives a spread in photon energy of $\pm 1\%$ at 0.3 eV, rising to $\pm 4\%$ at 0.03 eV.

Although it is unlikely that these systematic distortions of the data are responsible for the structure seen, we cannot rule out such a possibility.

In summary, the relativistic Doppler tuning of the barycentric photon energy of a CO₂ laser has enabled us to see, for the first time, the multiphoton photodetachment of H⁻ at a range of energies corresponding to the absorption of a minimum of three to eight photons. Preliminary yield curves are presented, although they do not necessarily represent the true structure of the cross section due to the large systematic uncertainties present in this first ex-

periment. It is planned to conduct a thorough survey of the cross section as a function of photon energy, laser intensity, and polarization, then examine the ATI phenomenon in a future experiment at LAMPF.

This work was performed under the auspices of the U.S. Department of Energy, in part under Grant No. DE-AS04-77ER03998, and was also supported in part by the U.S. Army Strategic Defense Command. We are grateful for the assistance and support of Jim Knudson, Bob Sander, Fred Archuleta, Jim Hontas, and George Kyrala. We wish to acknowledge helpful comments from Professor J. Eberly.

¹M. Crance and M. Aymar, *J. Phys. B* **18**, 3529 (1985).

²M. G. J. Fink and P. Zoller, *J. Phys. B* **18**, L373 (1985).

³G. P. Arrighini, C. Guidotti, and N. Durante, *Phys. Rev. A* **35**, 1528 (1987).

⁴R. Shakeshaft and X. Tang, *Phys. Rev. A* **36**, 3193 (1987).

⁵T. Mercouris and C. A. Nicolaides, *J. Phys. B* **21**, L285 (1988).

⁶P. Agostini and G. Petite, *Contemp. Phys.* **29**, 55 (1988), and references therein.

⁷C. L. Perkeris, *Phys. Rev.* **126**, 1470 (1962); M. Daskhan and A. S. Ghosh, *Phys. Rev. A* **28**, 2767 (1983); C. D. Lin, *Phys.*

Rev. Lett. **51**, 1348 (1983), and references therein.

⁸T. Mercouris and C. A. Nicolaides (unpublished).

⁹Lars Jönsson, *J. Opt. Soc. Am. B* **4**, 1422 (1987); P. H. Bucksbaum, M. Bashkansky, and T. J. McIlrath, *Phys. Rev. Lett.* **58**, 349 (1987).

¹⁰P. Lambropoulos, *Adv. At. Mol. Phys.* **12**, 87 (1976).

¹¹L. D. Landau and E. M. Lifshitz, *The Classical Theory of Fields*, 1st ed. (Addison-Wesley, Reading, MA, 1951), p. 122.